



Extended summary

Correlations among microstructure, effect of thermal
exposure and mechanical properties, in heat treated
Al-Si-Mg and Al-Cu aluminium alloys

Curriculum: Mechanical Engineering and Management

Author

Andrea Morri

Supervisor

Prof.ssa Lorella Ceschini

Curriculum Supervisor

Prof. Nicola Paone

Date: 30-January-2012



Abstract

Excellent aptitude to casting and forging processes, machinability, corrosion resistance and high strength-to-weight ratio, make heat treatable aluminium alloys suitable materials for various crucial applications in the automotive industry. However, the high strength levels achieved by the T6 heat treatment, are greatly influenced by the size, volume, and morphology of microstructural constituents, which in turn depend on composition, casting process and heat treatment procedure. Furthermore, in case of high temperatures exposure a loss of mechanical properties have to be considered too. All these issues often make a conservative approach necessary, with a consequent increase in thickness and weight. This work is part of a three years research project aimed to develop an innovative design procedure for cast engine parts where the process simulation of main microstructural parameters can lead to a mesh of corresponding mechanical properties for the structural simulation software. The aim of this work is to propose a physical, technological and mechanical characterisation of the EN AC-42100 T6 aluminium alloy used in the production of die cast cylinder heads and engine blocks. With the aim to support casting simulations, the study of the microstructure of the alloy and of its solidification behaviour was carried out. Optical microscopy, scanning electron microscopy and thermal analysis technique were employed. Concerning the support of structural simulations, the crucial aspects considered were the effects of the T6 heat treatment, the “preaging” and the thermal exposure on the mechanical properties of the alloy. Empirical equations with high determination coefficients were thus proposed to evaluate tensile and fatigue properties as a function of the crucial microstructural parameters and alloy hardness. Throughout the project, the presence of common problems in the design phase of cast (cylinder heads and engine blocks) and forged (pistons) components, has led to further studies on the thermal exposure behaviour of EN AW-4032 T6 and EN AW-2618 T6 wrought aluminium alloys.

Keywords

Al-Si-Mg, Castings, Forged Pistons, Mechanical Properties, Preaging, Thermal Exposure

1 Problem statement and objectives

Excellent aptitude to casting and forging processes, machinability, corrosion resistance and high strength-to-weight ratio, which increases performance and fuels economy, make heat treatable aluminium alloys suitable materials for various crucial applications in the automotive industry, such as engine blocks, pistons and cylinder heads [1-2]. The high strength levels are achieved by the T6 heat treatment that provides strengthening through the precipitation hardening mechanism [3]. T6 heat treatment consists in three fundamental steps: solution, quench and artificial aging (carried out in furnace). In the solution treatment the high temperatures promote the homogeneous diffusion of the hardening elements in the matrix. Through the water quench and subsequent artificial aging, a supersaturated matrix and a precipitation of hardening phases are respectively obtained. After the quench in fact, the supersaturated matrix, force the substitutional elements to form coherent precipitates reducing the total free energy of the system. These precipitates hinder the dislocation motion resulting in increased yield strength and hardness. However, the final hardness of the alloy results from the heat treatment parameters, such as time and temperature of the solution treatment, the quenching conditions and the artificial aging procedure. In the case of Al-Si-Mg casting alloys, also the short storage at room temperature between quenching and aging phases, due to the industrial handling of the components, is one of the crucial parameters affecting the tensile properties of the material [4]. This time, known as “preaging”, affects the precipitation sequence of metastable phases that occurs during the artificial aging. This sequence, for Al-Si-Mg alloys, can be summarised as follows: $\alpha(sss) \rightarrow \text{zone_GP} \rightarrow \beta'' \rightarrow \beta' \rightarrow \beta$ (Mg₂Si) [5]. In it, $\alpha(sss)$ is the supersaturated solid solution, GP zones are coherent Guiner-Preston zones, β'' are needle shaped precipitates associated with the peak-aged condition, β' rod shaped precipitates form after β'' precipitates in the aging sequence and β is the equilibrium phase [3,6]. To this sequence the literature usually attributes the hardness-time curve shown in Figure 1.

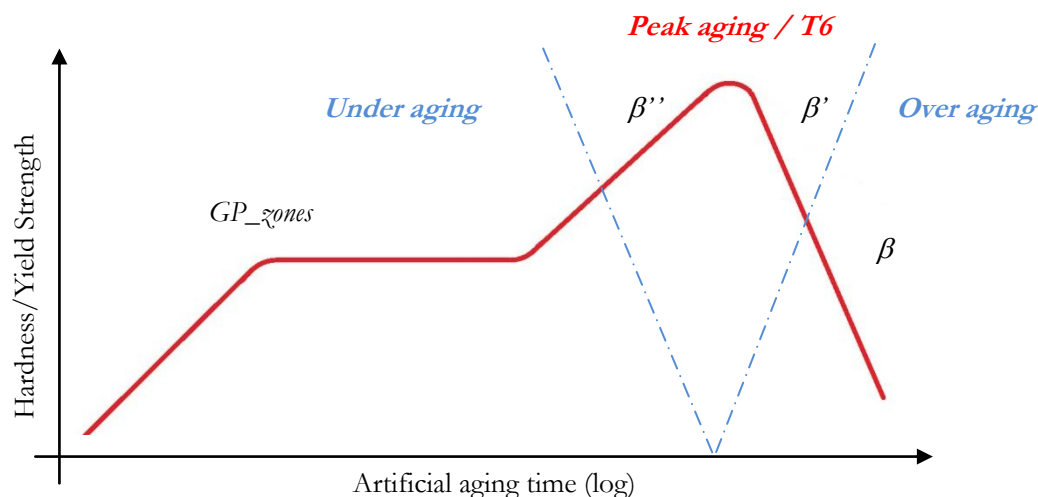


Figure 1. Hardness (Yield strength) as a function of artificial aging time (and associated precipitation hardening phases) for an Al-Si-Mg alloy.

However some recent studies, also based on the atom probe technique, have proposed different precipitation sequences concerning the formation of atomic clusters during the transition from α (sss) and β'' phase. On the base of the results obtained on Al-Mg-Si wrought alloys [7-10], it is supposed that the preaging greatly affects the clustering of Mg and Si atoms, leading thus to detrimental effects on mechanical properties after the heat treatment. Otherwise, the effects of preaging on mechanical properties and precipitation sequence of Al-Si-Mg casting alloy have not been enough studied in the past [4]. One of the main goals of this study was thus to evaluate the effect of natural pre-aging on the tensile properties of the EN AC-42100 T6 alloy, in order to evaluate/correct the heat treatment guidelines generally followed in industrial heat treatment practice and to better understand the effects of this phase of the heat treatment on the precipitation sequence that takes place during the aging. The final aim of this better understanding can be found in the need of high reproducibility of mechanical properties of the heat treated cast components. The designer, in fact, needs in turn to know as accurately as possible the mechanical properties of the material to best simulate its behaviour during the exercise, avoiding premature failure or excessive weight of the component.

A further consideration about the design of high thermo-mechanical stressed component such as cylinder heads, is the loss of mechanical properties with thermal exposure [3, 11]. Figure 1 qualitatively shows the loss of hardness (yield strength) as a consequence of the precipitation sequence from β'' to β phase and the subsequent change from Ashby to Orowan strengthening mechanism [3]. This loss often makes a conservative approach necessary when designing thermal stressed components, with a consequent increase in thickness and weight. The high temperatures reached in the combustion chamber [13] cause, in fact, the evolution of the precipitation sequence of intermetallic compounds involved in the precipitation hardening mechanism of the alloy. The literature reports instead the effects of the thermal exposure on hardness of as quenched heat treatable alloys, modelling its behaviour only for this condition [11, 14]. Otherwise, cast components are usually employed in T6 condition. Moreover, in all these cases, a constant exposure temperature is proposed while pistons or cylinder heads are subjected to variable temperatures depending on the engine working conditions. Models to evaluate the mechanical behaviour of an aluminium alloy as a function of exposure temperature and time, are available in literature but need in all cases experimental adjusting on the specific alloy. Moreover, this problem is common for both cast and wrought heat treatable aluminium alloys (such as those used for pistons forging). Always aiming at supporting the design phase of complex thermo-mechanically stressed components, a second goal of this research was thus to evaluate the evolution of tensile properties with thermal exposure of aluminium alloys. The effects of thermal exposure on mechanical properties of the as-quenched and T6 heat treated EN AC-42100 cast alloy and EN AW-2618 T6 and EN AW-4032 T6 wrought alloys were investigated.

In the case of complex cast components, such as gravity die cast heat treated Al-Si-Mg cylinder heads, the mechanical properties are greatly influenced by the size, volume, and morphology of microstructural constituents, which in turn depend on composition, casting process and heat treatment procedure [1, 15-17]. Usually, the microstructure of these components, consists of primary aluminium dendrites, eutectic Si, intermetallic compounds and solidifications defects such as gas pores, shrinkage cavities and oxides. Volume fractions of dendrites and eutectic Si are determined by the chemistry. Size, morphology and distribution of dendrites, eutectic Si and intermetallics compounds instead depend on the local so-

lification conditions too. As well known SDAS is in fact related to the solidification time (t_s) through the well-known relationship:

$$SDAS = k \cdot t_s^m \quad (1)$$

where k and m are material constants. Several works [15,16] report that the ultimate tensile strength and the elongation to failure are strongly affected by the primary and secondary dendrite arm spacing (DAS and SDAS). Moreover, they are also affected by the size and morphology of the eutectic Si, and by the presence of casting defects. The literature shows that UTS and E% increase when SDAS decreases and that small globular Si structures, induced for example by chemical modification, mainly enhance E%. However, it has been reported by Wang [16] that the relation between UTS, E% and SDAS is not linear for Al-Si-Mg age hardened alloys and, in particular, ductility does not always decrease as the dendrite cell size increases. As sad before, high values of yield strength and Brinell hardness are instead mainly influenced by the precipitation hardening induced by the T6 heat treatment process and practice [3,11,12]. Dendritic structures have in fact only an indirect effect on the heat treatment response. For example, the dissolution of smaller second phases during the solution treatment is easier for fine SDAS and consequently the higher solute concentration allows a more effective age hardening. The influence of eutectic Si and Fe-based intermetallic compounds on the tensile properties of Al-Si-Mg alloys was highlighted in several works [15,18]. If solidification defects are negligible, fracture occurs when the damage reaches a critical level and the failure follows three stages: i) cracking of the eutectic Si particles, at low plastic strains (1–2%); ii) generation of localized shear bands, with microcracks forming by joining adjacent cracked particles; iii) microcracks coalescence, followed by propagation, leading to the final fracture. The Si particle size and aspect ratio increasing, increases the probability of their fracture. Furthermore, clusters of particles favour both a high particle cracking rate and the coalescence of microcracks during the damage process. Fe-based intermetallics, especially π -Al₈Mg₃FeSi₆, have a similar behaviour and play an important role in the fracture of the alloys, if present in large volumes. All these issues have to be considered during the design of a complex Al-Si-Mg casting, because a variety of local microstructures, produced by different solidification conditions, can lead to a wide range of mechanical properties. For this reason, one of the goals of researchers over the last 40 years has been to relate the properties of Al alloy castings to their microstructure, in order to develop non-destructive test techniques that can predict the tensile properties of a casting from its microstructural characterization [19]. However, the proposed empirical equations did not consider the influence of solidifications defects on tensile properties. This assumption can be true only for the yield strength in the case of sound castings, because no substantial deformation occurs and the reduction of the loading area due to defects is negligible. On the contrary, UTS and E% are clearly affected by solidification defects, because the tensile failure propagates by plastic bridges between different defects, clearly reducing the amount of plastic deformation [15]. Furthermore, another weak point of some of the previously reported relations refers to the measurement of the microstructural parameters linked to the Si particles. As already sad, all these issues often make a conservative approach necessary, with a consequent increase in thickness and weight. Another aim of this work was therefore to develop simple experimental equations that can successfully predict the local tensile properties of complex Al-Si-Mg castings on the basis of some microstructural parameters and the hardness. Mechanical testing can be thus easily made even in

zones of the casting where tensile specimens cannot be extracted. A further and great advantage of this approach, is also the possibility to implement the model in a casting simulation software to evaluate the mechanical properties distribution just in the design phase of a cast component.

2 Research planning and activities

After a first evaluation of the state-of-the-art of casting processes, heat treatment procedure, microstructure and mechanical properties of Al-Si-Mg alloys, in order to achieve the intended goals, a physical, microstructural and mechanical characterization of EN AC-42100, EN AW-4032 and EN AW-2618 aluminium alloys (according to EN 1706 and EN 573-3 standards) was carried out. For all the alloys both the F (as fabricated) and the T6 (solutioned, quenched and artificially aged) states (according to EN 515 and EN 1706 standards) were considered and the experimental material was extracted directly from the industrial components shown in Figure 2.

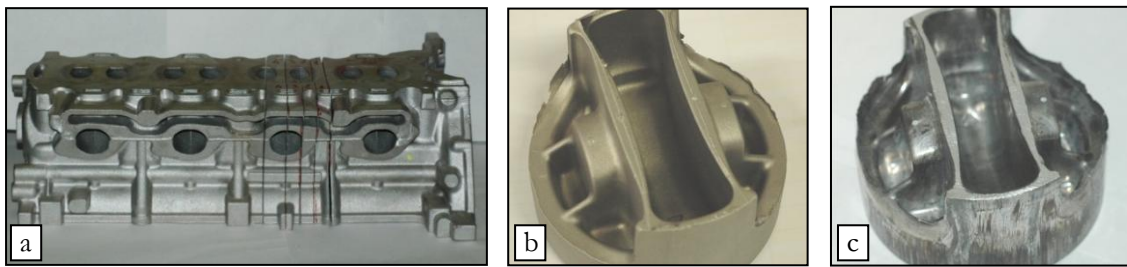


Figure 2. Experimental material: EN AC-42100 die cast cylinder head (a); EN AW-4032 and EN AW-2618 forged pistons (b and c respectively).

The physical characterisation of the alloys was performed through differential scanning calorimetry to indagate critical temperature of liquid-to-solid and solid-state phase transformations of the materials. Samples of about 50 mg were used in the analyses carried out with a heating/cooling rate of 10°C/min. As already said, different heat treatment conditions were tested.

For all the specimen tested, heat treatments were carried out by a high controlled (± 1 °C) electric furnace closely following (or not) the industrial guidelines and specifications. Water quenching was carried out, if necessary, by immersion in a thermostated water bowl.

The mechanical characterization of the aluminium alloys was performed through Brinell hardness, tensile and fatigue tests. The first were carried out with a 2.5 mm diameter ball and 62.5 kgf load according to ASTM E 10-08 standard. The second, according to UNI EN 10002 standard, were carried out (on a screw testing machine) at 25 °C and 250 °C, at a nominal strain rate of $3.3 \cdot 10^{-3} \text{ s}^{-1}$, using flat specimens with a 30 mm gauge length and a cross section of about 30 mm². Fatigue test were carried out according to ASTM E466-7 standard on a rotating bending fatigue machine at 50 Hz load frequency.

Fracture surfaces of the tensile and fatigue specimens were examined by using a scanning electron microscope (SEM). Metallographic samples preparation was achieved by standard metallographic techniques, including mechanical grinding, polishing and etching. Micro-

structural analyses were carried out by SEM, optical microscopy (OM) and digital image analysis (IA).

Statistical Analysis and calculations were carried out by using spreadsheets and a statistical analysis software (*XLStat*[®]). Correlation matrices and multiple variable correlation analysis tools were employed. A MATLAB[®] routine has been then developed for the calculation of the residual mechanical properties of a generic T6 heat treated alloy after thermal exposure with changing in temperatures.

3 Analysis and discussion of main results

Tensile and hardness tests on specimens extracted from some EN AC-42100 T6 die cast cylinder heads show how a great range of mechanical properties can be obtained in the same casting and in castings belonging to different batches of production. OM, SEM and IA techniques were used to investigate the microstructure of tensile specimens. SDAS ranges from 25 μm to 70 μm depending on the local solidification conditions. Low hydrogen content of the melt (0.18 $\text{cm}^3/100\text{ g}$) and optimized process parameters resulted in very low solidification defect content (0%÷5%). The reduced Fe content in the primary Al alloy used in the industrial casting process and the addition to the melt of small amounts of Mn, result in very low contents of Fe-rich intermetallic compounds. Their shape and area (10÷90 μm^2) ranges were due to the local solidification conditions. The effects of secondary alloying element such as Ti, B and Sr on grain size and eutectic Si size were evaluated. Both of them were near constant in the castings ranging from about 300 μm to 600 μm and from 8 μm^2 to 19 μm^2 respectively. Empirical correlations between some of these microstructural features, the hardness and the tensile properties of the EN AC-42100 T6 alloy were proposed:

$$YS = 3.419 \cdot BH - 127.6 \quad (2)$$

$$UTS = 0.183 \cdot SR\%^{0.803} \cdot SDAS^{-0.121} \cdot BH^{0.888} \quad (3)$$

$$E\% = 5074.8 \cdot SR\%^{2.951} \cdot SDAS^{-1.239} \cdot BH^{-2.857} \cdot A^{-0.957} \quad (4)$$

where YS = yield strength (0,2% proof strength, MPa); BH = Brinell Hardness; UTS = Ultimate tensile strength (MPa); SR% = fraction of defect free fracture surface (%); SDAS = Secondary dendrite arm spacing (μm); E% = Elongation to failure (%); A = average area of eutectic silicon (μm^2). A very high determination coefficient ($R^2 = 0.91$) was found for the linear relationship between hardness and yield strength (Eq. 1) confirming the primary role of the heat treatment in defining these properties. With regard to the influence of microstructural parameters, SDAS and area fraction of solidification defects affected both ultimate tensile strength and elongation to failure. Determination coefficient values resulted in 0,90 and 0,81 for Equation 3 and Equation 4 respectively. The predictive models for YS and UTS led to an average error between the predicted values and the experimental ones of only about 2%, while large data scatter characterized the elongation to failure, with an average error of about 20%. The evaluation of more microstructural parameters than in the past, results in an increased accuracy of the new empirical models respect to those previ-

ously proposed [19] but their use only to limited ranges of variation of the considered input variables has to be taken into account.

Confirming the literature data [20], the results of rotating bending fatigue tests show high data dispersion for low stress levels, while good correlations ($R^2 \cong 0,6$) with SDAS and average defect content were observed for the higher ones (70 MPa). Equation 5 and Equation 6 report the numerical relationship between cycles to failure and percentage defect content (%DC) and SDAS respectively. This is an important finding if it is considered that commercial casting simulation software can nowadays simulate SDAS and fraction amount of solidification defects distributions of a casting. However, a clear explanation of the high data dispersion typical of low stress levels tests was not found since any attempt to correlate the fatigue life of the specimens to the size and position of the defects acting as crack initiator was unsuccessful. A partial explanation of such a behaviour, as instead be found in the presence of multiple crack initiations on the same fracture surface. However, the interaction among multiple defects has still to be completely understood.

$$Nf = 4 \cdot 10^6 \cdot e^{-2.49\%DC} \tag{5}$$

$$Nf = 3 \cdot 10^{11} \cdot e^{-0.25 \cdot SDAS} \tag{6}$$

The effects of the thermal exposure on the mechanical properties of the EN AC-42100 aluminium casting alloy were first studied through Brinell hardness tests. Constant hardness curves were defined for both the as-quenched and the T6 alloys (Fig. 3). The hardness data obtained from the as-quenched alloy (Fig. 3a) confirmed those reported in literature [11], while those obtained for the T6 condition (Fig. 3b) were discussed considering the results of differential scanning calorimetry (DSC) analyses. In this second case, it is clear how the experimental data reported in Figure 3b provide a simple instrument for a reverse-engineering approach to evaluate the working temperature of the component after a defined endurance bench test. For a given time, the evaluation of the local hardness of the material, gives in fact its average working temperature and can thus support CFD simulations of temperature distribution in the component.

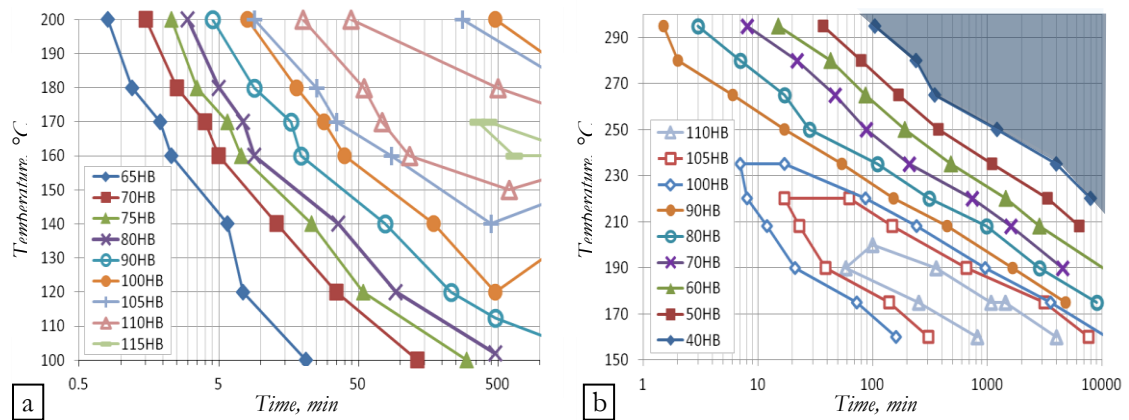


Figure 3. Constant hardness curves for the as quenched (a) and the T6 (95BH) (b) EN AC-42100 aluminum alloy. Blue area of figure b represents an hardness plateau (40 BH).

Figure 3 (a and b) clearly shows that: i) 115 Brinell represent the peak aging condition of the material; ii) the industrial heat treatment is carried out to reach a under aged (95 BH) condition. The hardness of the castings can thus increase or decrease with further thermal exposure depending on the exposure temperature (Fig. 3b). Tensile tests were carried out to evaluate the relationship between tensile properties and residual hardness of the material. Different exposure temperatures and times were used to cover the entire range of variation of hardness (45÷115 BH). Like Tiryakioglu et al. [12] a linear relationship between yield strength and Brinell hardness was found with no effects of SDAS on this mechanical property. Original results were instead obtained for the ultimate tensile strength and the elongation to failure (Fig. 4). It is clear how, in the over aged condition, and in opposition to what stated before, SDAS doesn't seem to affect UTS. In Figure 4a in fact, there are not any differences between fine (25÷40 μm) and large (55÷70 μm) SDAS data. Elongation to failure seems instead greatly affected both by SDAS and residual hardness of the alloy. Higher values were always obtained for fine SDAS specimens with further increase with lower hardness values.

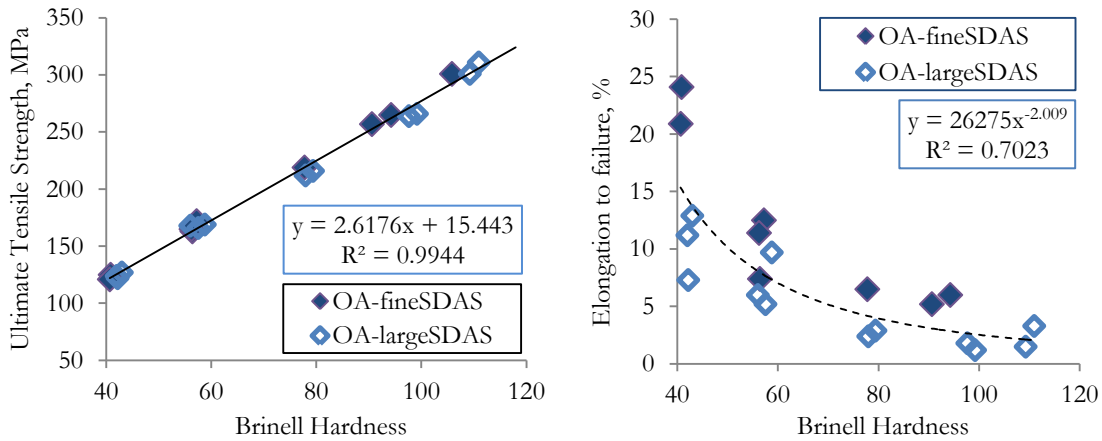


Figure 4. Ultimate tensile strength and elongation to failure as a function of Brinell hardness of the EN AC-42100 T6 alloy in the over aged (and peak aged) conditions. Fine (25÷40 μm) and large (55÷70 μm) SDAS specimens were tested.

A similar behaviour was also observed for the EN AW-2618 T6 and EN AW-4032 T6 wrought alloys. The tensile tests and data analyses, allowed to define ultimate tensile strength, yield strength, elongation to failure, strength coefficient (K) and strain hardening exponent (n) as a function of the hardness of the alloys. Also for the high temperature (250 °C) tests, very high determination coefficients were obtained ($R^2 \cong 0.9$). The effects of the microstructure on mechanical properties of these alloys result only in a maximum 5% variation depending on the extraction zone of the specimens. The collected results were used to define a simple model for simulate the true stress-strain behaviour of the materials (Equation 7 for EN AW-2618 T6 and Equation 8 for EN AW-4032 T6 alloys).

$$\sigma_r = (0,56 \cdot BH + 512) * \varepsilon_r^{(-0.0029 \cdot HB + 0.4848)} \quad (7)$$

$$\sigma_r = (3,01 \cdot BH + 159) * \varepsilon_r^{(-0.0018 \cdot HB + 0.3252)} \quad (8)$$

During the evaluation of the accuracy of the industrial T6 heat treatment guidelines for the EN AC42100 cast alloy, the effect of the delay between quenching and aging was considered. Differential scanning calorimetry (DSC) analyses on solutioned, quenched and 0÷96h pre-aged samples, suggested that the nature and composition of the clusters formed during pre-aging, influence the subsequent precipitation process and the final mechanical properties of the alloy. These results were also confirmed by tensile and hardness test data, with a decrease in both yield and ultimate tensile strengths with increased pre-aging time. Figure 5 reports the DSC patterns for differently preaged specimens together with the precipitation sequence proposed by Serizawa [10]. Figure 6 shows the effect of the preaging on the ultimate tensile strength of the material.

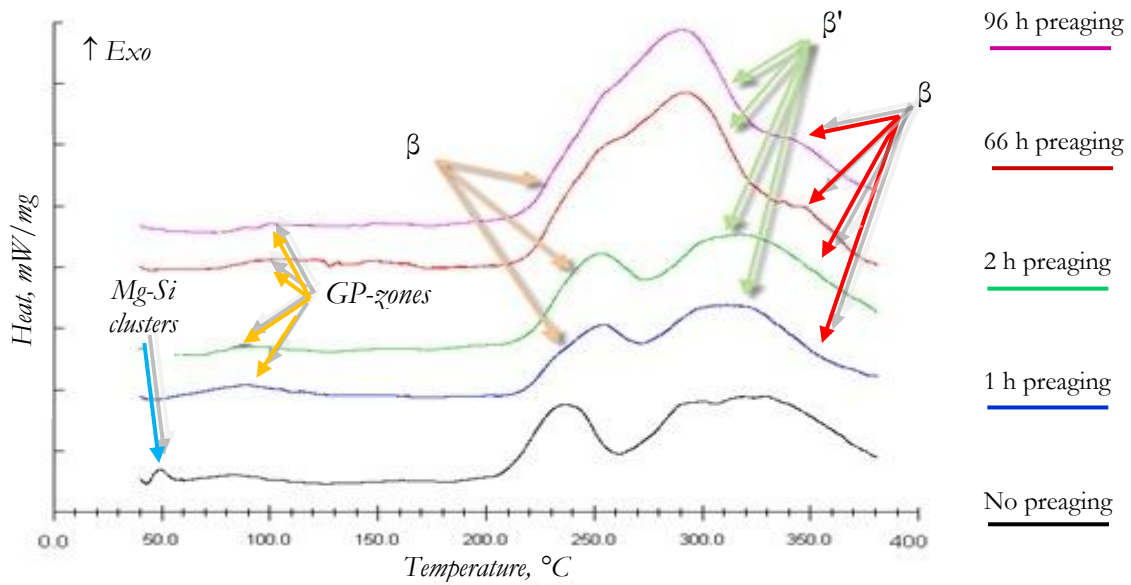


Figure 5. DSC patterns (10 °C/min) for as quenched and differently preaged samples of EN AC-42100 aluminum alloy.

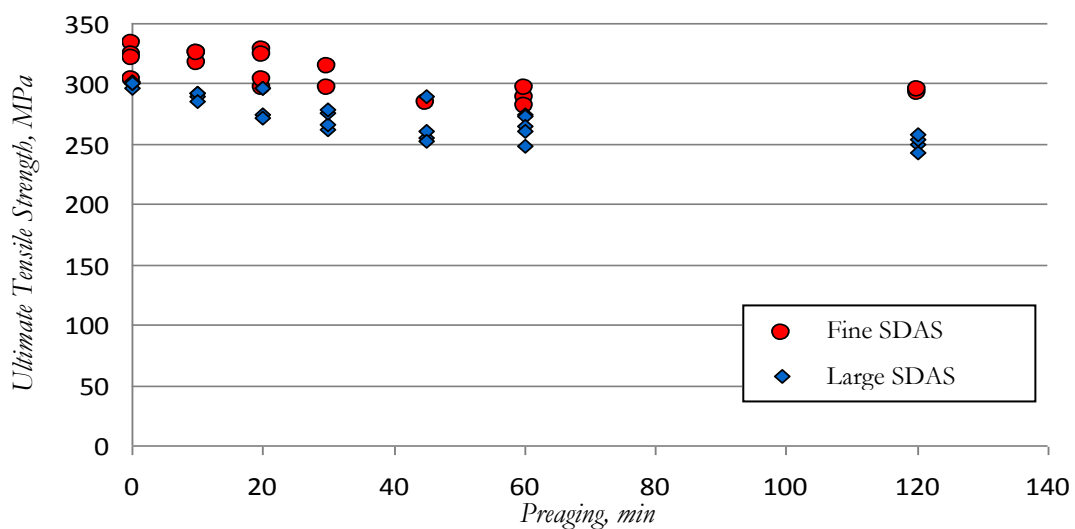


Figure 6. UTS behaviour of fine (25±40 μm) and large (55±70 μm) SDAS EN AC-42100 T6 specimens as a function of preaging.

It is clear how two hours of pre-aging were responsible for about 15% reduction in UTS. Moreover, SDAS confirms its crucial role in the plastic deformation of the material leading to higher UTS values when finer. A similar behaviour was observed for hardness and yield strength data. However, in these cases no effects of SDAS were observed. Elongation to failure data show instead that increased preaging time leads to higher values only for fine SDAS specimens. By considering all the tensile properties and hardness values, it was clearly observed that, in the industrial practice (artificial aging of 4,5 h at 165 °C), more than 20 min preaging time leads to under aging of the alloy. SDAS and hardness were identified as crucial variables to evaluate the tensile behaviour of the material. Empirical models with high determination coefficients ($R^2 \cong 0,8$) were proposed to evaluate UTS, YS, E%, K and n of the alloy in the under aged and peak aged conditions. Finally, the equations providing the mechanical properties of the EN AC-42100 T6 alloy as a function of its hardness for under and over aged conditions and fine or large SDAS are shown in Table 1. To underline the original contribution of the work and the accuracy of the models, a comparison between the simulated and true mechanical behaviour of the material is reported in Figure 7. In it, average SDAS, different hardness and under and over aged conditions specimens are considered.

At the end of the study, in order to evaluate the reliability of the experimental data, a MATLAB® routine has been developed for the calculation of the residual mechanical properties of a generic heat treatable alloy after thermal exposure with changing in temperatures. The results obtained with constant-temperature tests were confirmed by the experiments (4% max error), while worse results were obtained with variable-temperatures tests. However, these results are believed to have large margin for improvement.

Table 1. Mechanical properties models and relative determination coefficients for different class of SDAS and aging conditions of the EN AC-42100 T6 cast alloy.

Mechanical Property	Under aged (90 < BH < 115)		Over aged (40 < BH < 115)	
	SDAS 25÷40 µm	SDAS 55÷70 µm	SDAS 25÷40 µm	SDAS 55÷70 µm
Rp0,2 [MPa]	3.505*BH – 135.5 R ² = 0.8461	3.212*BH – 107.2 R ² = 0.9364	2.990*BH – 59.1 R ² = 0.9962	2.966*BH – 55.1 R ² = 0.9946
UTS [MPa]	2.039*BH + 89.6 R ² = 0.6400	2.470*BH + 17.9 R ² = 0.7976	2.689*BH + 13.5 R ² = 0.9983	2.589*BH + 15.4 R ² = 0.9951
E%	-0.346*BH + 47.6 R ² = 0.6969	-0.040*BH + 7.6 R ² = 0.0315	9360*BH ^{-1.66} R ² = 0.8756	15501*BH ^{-1.949} R ² = 0.8052
C [MPa]	0.63*BH + 375 R ² = 0.1245	1.43*BH + 270 R ² = 0.5527	2.82*BH + 108 R ² = 0.9632	3.03*BH + 100 R ² = 0.9569
n	-0.0027*BH + 0.41 R ² = 0.8091	-0.002*BH + 0.32 R ² = 0.8877	-0.0018*BH + 0.26 R ² = 0.9513	-0.0017*BH + 0.26 R ² = 0.9535

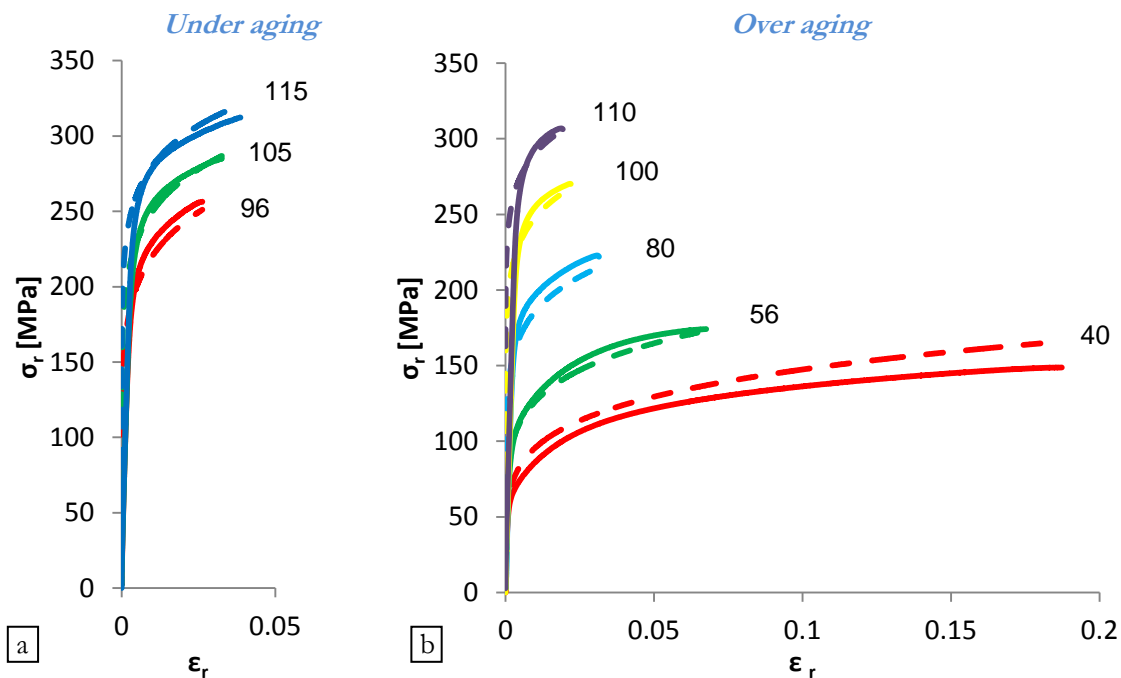


Figure 7. Simulated (dotted) and measured (solid) true stress-strain curves of EN AC-42100 T6 tensile specimens. The behaviours of about $45 \mu\text{m}$ SDAS, different Brinell hardness and under (a) and over (b) aged specimens are shown.

4 Conclusions

This work is part of a research project aimed to propose an innovative design procedure for cast engine parts where the process simulation of the main microstructural parameters can lead to a mesh of corresponding mechanical properties available for the structural simulation software. Moreover, the latter needs to implement a model of the material that takes into account the effects of high thermo-mechanical stress conditions on the mechanical properties of the material itself. Nowadays it is believed that the great use of simulations can support the designer to reduce both the cost and the time to market of new products and overcoming thus the challenges posed by the rising economic powers. To make this true, process and structural simulation software have to provide reliable and accurate results. A huge experimentation on processes and materials to develop reliable models has thus to be carried out. In this context, this work has been in turn carried out to further understand the mechanical behavior of some aluminum heat treatable alloys involved in the production of high performance engine components. The main scientific contributions of this work can be summarised as follows:

- Natural preaging greater than 20 minutes greatly affects the precipitation sequence of Mg-Si strengthening phases in the EN AC-42100 T6 cast alloy. The hardness and the tensile properties of the material are, in turn, detrimental affected.
- Tensile properties of the EN AC-42100 T6 cast alloy greatly depends on its hardness, defect content, SDAS and size of eutectic Si.
- Reliable empirical models to evaluate ultimate tensile strength, yield strength, and elongation to failure of the under aged and peak aged EN AC-42100 T6 cast alloy were proposed.

- Fatigue life of EN AC-42100 T6 cast alloy is affected by high data scatter and seems to depend on SDAS and defect content only when high stress amplitudes are applied.
- High accuracy (hardness and SDAS based) models were proposed to evaluate ultimate tensile strength, yield strength, elongation to failure, strength coefficient and strain hardening exponent of the EN AC-42100 T6 cast alloy after thermal exposure.
- Similar models were also developed for the EN AW-2618 T6 and EN AW-4032 T6 wrought alloys.
- The high temperature tensile behaviour (250°C) seems to replicate the room temperature one highlighting a linear dependence of UTS from residual hardness and a very high determination coefficient also for Hardness-Elongation to failure relationship.
- A *MATLAB*[®] routine for the simulation of the residual mechanical properties of a generic heat treatable alloy after thermal exposure with changing in temperatures has been developed: the obtained results suggest a large margin for future improvements

References

- [1] J. G. Kaufman and E. L. Rooy, *Aluminium alloy castings, Properties, Processes and applications*, ASM International, 2004.
- [2] L. Ceschini, Al. Morri, An. Morri and G. Pivetti, *Predictive equations of the tensile properties based on alloy hardness and microstructure for an A356 gravity die cast cylinder head*, *Materials and design*, vol. 32 pp. 1367–1375, 2011.
- [3] M. H. Jacobs, *Precipitation Hardening*, TALAT Lecture 1204, European Aluminium Association, 1999.
- [4] S. Shivkumar, C. Keller and D. Apelian, *Aging Behavior in Cast Al-Si- Mg Alloys*, AFS Transactions, vol. 98, pp. 905-911, 1990.
- [5] J. Lendvai, T. Ungár and I. Kovács, *The Effect of the Temperature of Solution Treatment and Quenching on the Zone Formation Process in Al-Mg-Si Alloys*, *Materials Science and Engineering*, vol. 16, pp. 85-89, 1974.
- [6] I. Dutta and S. M. Allen, *A calorimetric study of precipitation in commercial aluminium alloy 606*, *Journal of Materials Science Letters*, vol. 10, pp. 323-326, 1991.
- [7] G.A. Edwards, K. Stiller, G. L. Dunlop and M. J. Couper, *The precipitation sequence in Al-Mg-Si alloys*, *Acta materialia*, vol. 46, pp. 3893-3904, 1998.
- [8] M. Murayama and K. Hono. *Pre-precipitate clusters and precipitation processes in Al-Mg-Si alloys*, *Acta materialia*, vol. 47, pp. 1537-1548, 1999.
- [9] F. De Geuser, W. Lefebvre and D. Blavette. *3D atom probe investigation of solute atoms clustering during natural ageing or preageing in an AlMgSi alloy*, *Philosophical Magazine Letters*, vol. 86, pp. 227 – 234, 2006.
- [10] A. Serizawa, S. Hirose and T. Sato. *Three-Dimensional Atom Probe Characterization of Nanoclusters Responsible for Multistep Aging Behavior of an Al-Mg-Si Alloy*, *Metallurgical and Materials Transactions A*, vol. 39, pp. 243-251, 2008.
- [11] P.A. Rometsch and G.B. Schaffer; *An age hardening model for Al-7Si-Mg casting alloys*, *Materials Science and Engineering A*, vol. 325, pp. 424–434, 2002.
- [12] Murat Tiryakioğlu, John Campbell and James T. Staley, *On macrohardness testing of Al-7% Si-Mg alloy II. An evaluation of models for hardness-yield strength relationship*, *Materials Science and Engineering A*, vol. 361, pp. 240–248, 2003.
- [13] L. Ceschini, G. Nicoletto, E. Riva, A. Strozzi and L. Tomesani, *Proceedings of 1° Congresso Nazionale del Coordinamento della Meccanica Italiana*, Palermo, 2010.
- [14] Deschamps A and Brechet Y, *Influence of predeformation and ageing of an Al-Zn-Mg alloy - II. Modeling of precipitation kinetics and yield stress*, *Acta Materialia*, vol. 47, pp. 293-305, 1999.

- [15] J. Campbell, *CASTINGS, The new metallurgy of cast metals*, Butterworth-Heinemann Edition, 2nd Edition, 2003.
- [16] Q.G. Wang, *Micro structural effect on the tensile and fracture behaviour of aluminium casting alloy A 356/357*, Metallurgical and Materials Transactions A, vol. 34, pp.2887-2899, 2003.
- [17] Q. G. Wang, D. Apelian and D. A. Lados, *Fatigue Behavior of A356-T6 Aluminum Cast Alloy. Part II. Effect of Microstructural Constituents*, Journal of Light Metals, vol. 1, pp. 85-97, 2001.
- [18] J.A. Taylor, *The effect of iron in Al-Si casting alloys*, Proceedings of Australian Foundry Institute National Conference, Birsbane. 2004.
- [19] M. Drouzy, S. Jacob and M. Richard, *Interpretation of Tensile Results by Means of Quality Index and Probable Yield Strength*, AFS International Cast Metals Journal, pp. 43-50 ,1980.
- [20] I. Boromei, L. Ceschini, Alessandro Morri, Andrea Morri, G. Nicoletto and E. Riva, *Metallurgical Science and Tecnology*, vol. 28, pp. 18-24, 2010.